Charge-conserving grid based methods for the Vlasov–Maxwell equations

Nicolas Crouseilles, Pierre Navaro, Eric Sonnendrücker

Charge conserving grid based methods for the Vlasov-Maxwell equations

Nicolas Crouseilles[a], Pierre Navaro[b], Eric Sonnendrücker[c,d]

[a]*Inria-Rennes Bretagne Atlantique, IPSO Project*
[b]*IRMA – CNRS & Université de Strasbourg*
[c]*Max-Planck Institute for plasma physics, Boltzmannstr. 2, D-85748 Garching*
[d]*Mathematics Center, TU Munich, Boltzmannstr. 3, D-85747 Garching*

Abstract

In this article we introduce numerical schemes for the Vlasov-Maxwell equations relying on different kinds of grid based Vlasov solvers, as opposite to PIC schemes, that enforce a discrete continuity equation. The idea underlying this schemes relies (see [14]) on a time splitting scheme between configuration space and velocity space for the Vlasov equation and on the computation of the discrete current in a form that is compatible with the discrete Maxwell solver.

Keywords: Maxwell-Vlasov system, discrete continuity equation, Finite Volume method, Spectral method, semi-Lagrangian method

1. Introduction

We consider the motion of particles in their self-consistent electromagnetic field, which can be described by the Vlasov-Maxwell equations. In this work, we restrict ourselves to the two-dimensional non relativistic model, which involves four phase space dimensions, namely x, y, v_x, v_y, but the ideas developed here can be extended in a straightforward manner to the 3D relativistic model. In our case the unknown quantities are the particle distribution function $f(t, \mathbf{x}, \mathbf{v})$, the electric field $\mathbf{E}(t, \mathbf{x}) = (E_x, E_y, 0)$ and the magnetic field $\mathbf{B}(t, \mathbf{x}) = (0, 0, B_z)$, where we denote by $\mathbf{x} = (x, y)$ and $\mathbf{v} = (v_x, v_y)$. Then the Vlasov equation reads

$$\frac{\partial f}{\partial t} + \mathbf{v} \cdot \nabla_{\mathbf{x}} f + (\mathbf{E}(t, \mathbf{x}) + \mathbf{v} \times \mathbf{B}(t, \mathbf{x})) \cdot \nabla_{\mathbf{v}} f = 0, \tag{1}$$

where $\nabla_{\mathbf{x}}$ denotes the gradient in configuration space and $\nabla_{\mathbf{v}}$ denotes the gradient in velocity space. The initial condition $f(0, \mathbf{x}, \mathbf{v}) = f_0(\mathbf{x}, \mathbf{v})$ is given. The self-consistent electromagnetic field $(\mathbf{E}(t, \mathbf{x}), \mathbf{B}(t, \mathbf{x}))$ is computed thanks to Maxwell's equations

$$\frac{\partial \mathbf{E}}{\partial t} - \nabla_{\mathbf{x}} \times \mathbf{B} = -\mathbf{J}, \tag{2}$$

$$\frac{\partial \mathbf{B}}{\partial t} + \nabla_{\mathbf{x}} \times \mathbf{E} = 0, \tag{3}$$

$$\nabla_{\mathbf{x}} \cdot \mathbf{E} = \rho, \tag{4}$$

$$\nabla_{\mathbf{x}} \cdot \mathbf{B} = 0. \tag{5}$$

The source of Maxwell's equations, namely the charge density ρ and current density $\mathbf{J} = (J_x, J_y)$ are computed from the particle distribution f and the uniform neutralizing Maxwellian background particles defined by their density $n_b(\mathbf{x}) = \int f_0(\mathbf{x}, \mathbf{v})\, d\mathbf{v}$ thanks to

$$\rho(t, \mathbf{x}) = \int_{\mathbb{R}^2} f(t, \mathbf{x}, \mathbf{v})\, d\mathbf{v} - n_b(\mathbf{x}), \qquad \mathbf{J}(t, \mathbf{x}) = \int_{\mathbb{R}^2} f(t, \mathbf{x}, \mathbf{v}) \mathbf{v}\, d\mathbf{v}. \tag{6}$$

Note that integrating the Vlasov equation (1) with respect to the velocity variable $\mathbf{v}$ yields

$$\frac{\partial \rho}{\partial t} + \nabla_{\mathbf{x}} \cdot \mathbf{J} = 0, \tag{7}$$

which is called the continuity equation and expresses the local conservation of charge. In the continuous setting, provided this continuity equation is satisfied and Gauss' law (4) is satisfied at time $t = 0$, if the electric and magnetic fields are computed using only Ampère's law (2) and Faraday's law (3), Gauss' law is satisfied for all time. In general, numerical Vlasov-Maxwell solvers being PIC, Eulerian or semi-Lagrangian do not verify this and a correction scheme is generally used to enforce Gauss' law at each time step or from time to time.

The aim of this paper is to propose a general procedure, valid for Vlasov solvers on a cartesian grid based on a splitting method between configuration and velocity space, that enables to establish a discrete continuity equation verified by the discrete charge and current densities computed from the Vlasov solver compatible with the Maxwell solver, so that only Ampère's and Faraday's law will need to be advanced by our Maxwell solver, Gauss' law being a consequence of those.

A number of work has been proposed to tackle this problem in PIC solvers (see [16, 4, 15, 12, 11, 1, 2]) but also in the Eulerian case. In this latter case, one can cite [10] in which charge is preserved using a forward semi-Lagrangian Vlasov solver and [14] in which a conservative PPM method is used in such a way that the Gauss law is ensured. The present work combines ideas of [14] and [9]. Indeed, in [9], a general framework for conservative semi-Lagrangian methods is proposed so that [14] can be generalized to a class of Vlasov solvers. We also mention [7] in which a Hamiltonian splitting is proposed for the Vlasov-Maxwell equations that enables to derive charge preserving high order in time methods.

The outline of the paper is as follows. First we will derive the discrete continuity equations associated to the Yee Maxwell solver and to a spectral solver, then we will introduced an algorithm for computing the discrete charge and current densities compatible with these discrete continuity equations for a conservative semi-Lagrangian algorithm and a spectral algorithm. Finally, after presenting the coupling algorithm, we will validate our method on some relevant test cases.

2. Discrete continuity equations

A discrete continuity equation is necessarily linked to the Maxwell solver, as the discrete curl and divergence operators need to be compatible. To this aim a first requirement of the Maxwell solver, is that the discrete divergence of the discrete curl vanishes. In this case a discrete continuity equation specific for each solver can be derived such that if this discrete continuity equation is satisfied and the Gauss law is satisfied at time step $t^n = n\Delta t$ it will also be satisfied at time step t^{n+1}.

The formulation of the discrete continuity equation for the Yee scheme, as well as for Finite Volume schemes for the Maxwell system on unstructured grids with the leap-frog and other time stepping schemes have already been obtained by Bouchut [3].

We shall recall here the discrete continuity equation for the classical Yee solver and also introduce it for a spectral solver associated to a leap-frog method in time.

2.1. For the Yee Maxwell solver

Let us first consider the classical Yee solver on a staggered mesh. First, we introduce a mesh in the x and y directions: $x_i = x_{\min} + i\Delta x$, $\Delta x =$

$(x_{\max} - x_{\min})/N_x$ and $y_j = y_{\min} + j\Delta y$, $\Delta y = (y_{\max} - y_{\min})/N_y$. Then, we define the center of the cells $x_{i+1/2} = x_i + \Delta x/2$ and $y_{j+1/2} = y_j + \Delta y/2$. We also introduce the time discretization: $t^n = n\Delta t$, $n \in \mathbb{N}, \Delta t > 0$, and $t^{n+1/2} = t^n + \Delta t/2$. The Yee scheme is satisfied by

$$\begin{aligned} E^n_{x_{i+1/2,j}} &\simeq E_x(t^n, x_{i+1/2}, y_j), \\ E^n_{y_{i,j+1/2}} &\simeq E_y(t^n, x_i, y_{j+1/2}), \\ B^{n-1/2}_{z_{i+1/2,j+1/2}} &\simeq B_z(t^{n-1/2}, x_{i+1/2}, y_{j+1/2}), \end{aligned}$$

for a given current $J^{n+1/2}_{x_{i+1/2,j}} \simeq J_x(t^{n+1/2}, x_{i+1/2}, y_j)$ and $J^{n+1/2}_{y_{i,j+1/2}} \simeq J_y(t^{n+1/2}, x_i, y_{j+1/2})$. Figure 1 displays the positons of the different components of the fields on a staggered cartesian grid in the Yee scheme.

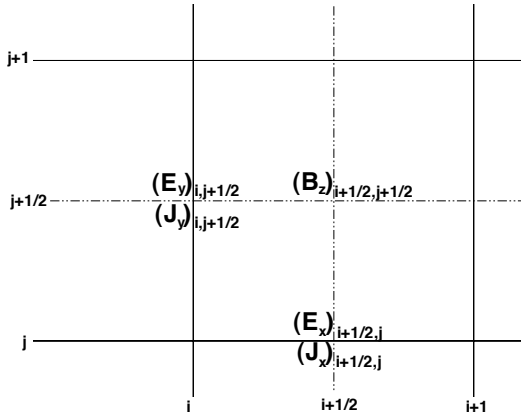

Figure 1: Positions of the different components of the fields in the Yee scheme.

The Yee scheme approximating (2)-(3) reads

$$\frac{E^{n+1}_{x_{i+1/2,j}} - E^n_{x_{i+1/2,j}}}{\Delta t} = \frac{B^{n+1/2}_{z_{i+1/2,j+1/2}} - B^{n+1/2}_{z_{i+1/2,j-1/2}}}{\Delta y} - J^{n+1/2}_{x_{i+1/2,j}}, \tag{8}$$

$$\frac{E^{n+1}_{y_{i,j+1/2}} - E^n_{y_{i,j+1/2}}}{\Delta t} = -\frac{B^{n+1/2}_{z_{i+1/2,j+1/2}} - B^{n+1/2}_{z_{i-1/2,j+1/2}}}{\Delta x} - J^{n+1/2}_{y_{i,j+1/2}}, \tag{9}$$

$$\frac{B^{n+1/2}_{z_{i+1/2,j+1/2}} - B^{n-1/2}_{z_{i+1/2,j+1/2}}}{\Delta t} = \frac{E^n_{x_{i+1/2,j+1}} - E^n_{x_{i+1/2,j}}}{\Delta y} - \frac{E^n_{y_{i+1,j+1/2}} - E^n_{y_{i,j+1/2}}}{\Delta x}. \tag{10}$$

The associated discrete Gauss' law at time t^n will then read

$$\frac{E^n_{x_{i+1/2,j}} - E^n_{x_{i-1/2,j}}}{\Delta x} + \frac{E^n_{y_{i,j+1/2}} - E^n_{y_{i,j-1/2}}}{\Delta y} = \rho^n_{i,j}. \tag{11}$$

Now, taking the discrete divergence of Ampère's law (8)-(9) yields

$$\frac{1}{\Delta t}\left(\frac{E^{n+1}_{x_{i+1/2,j}} - E^{n+1}_{x_{i-1/2,j}}}{\Delta x} + \frac{E^{n+1}_{y_{i,j+1/2}} - E^{n+1}_{y_{i,j-1/2}}}{\Delta y} - \frac{E^{n}_{x_{i+1/2,j}} - E^{n}_{x_{i-1/2,j}}}{\Delta x} - \frac{E^{n}_{y_{i,j+1/2}} - E^{n}_{y_{i,j-1/2}}}{\Delta y}\right) = -\left(\frac{J^{n+1/2}_{x_{i+1/2,j}} - J^{n+1/2}_{x_{i-1/2,j}}}{\Delta x} + \frac{J^{n+1/2}_{y_{i,j+1/2}} - J^{n+1/2}_{y_{i,j-1/2}}}{\Delta y}\right). \tag{12}$$

Let us now introduce, at time step t^n the following discrete continuity

$$\frac{\rho^{n+1}_{i,j} - \rho^n_{i,j}}{\Delta t} + \frac{J^{n+1/2}_{x_{i+1/2,j}} - J^{n+1/2}_{x_{i-1/2,j}}}{\Delta x} + \frac{J^{n+1/2}_{y_{i,j+1/2}} - J^{n+1/2}_{y_{i,j-1/2}}}{\Delta y} = 0. \tag{13}$$

If this is satisfied, it follows from (12) that

$$\frac{1}{\Delta t}\left(\frac{E^{n+1}_{x_{i+1/2,j}} - E^{n+1}_{x_{i-1/2,j}}}{\Delta x} + \frac{E^{n+1}_{y_{i,j+1/2}} - E^{n+1}_{y_{i,j-1/2}}}{\Delta y} - \frac{E^{n}_{x_{i+1/2,j}} - E^{n}_{x_{i-1/2,j}}}{\Delta x} - \frac{E^{n}_{y_{i,j+1/2}} - E^{n}_{y_{i,j-1/2}}}{\Delta y}\right) = \left(\frac{\rho^{n+1}_{i,j} - \rho^n_{i,j}}{\Delta t}\right).$$

So, if the discrete Gauss law (11) is satisfied at time t^n, it follows that

$$\frac{E^{n+1}_{x_{i+1/2,j}} - E^{n+1}_{x_{i-1/2,j}}}{\Delta x} + \frac{E^{n+1}_{y_{i,j+1/2}} - E^{n+1}_{y_{i,j-1/2}}}{\Delta y} = \rho^{n+1}_{i,j},$$

which is the discrete Gauss law at time t^{n+1}.

2.2. For a spectral Maxwell solver

We consider periodic boundary conditions in x and y so that discrete Fourier transform is adapted to the spatial discretization of the Vlasov and the Maxwell's equations. We denote by E^n_{x,k_x,k_y} the spatial discrete Fourier transform of $E_x(t^n)$ (similar notations are used for E_y, B_z, ρ, J_x and J_y),

with $t^n = n\Delta t$, $n \in \mathbb{N}, \Delta t > 0$. Then the Fourier transform in (x, y) of the Faraday and Ampère's equations together with a leap-frog scheme in time lead to the following Maxwell solver:

$$\frac{E^{n+1}_{x,k_x,k_y} - E^n_{x,k_x,k_y}}{\Delta t} = ik_y B^{n+1/2}_{z,k_x,k_y} - J^{n+1/2}_{x,k_x,k_y}, \tag{14}$$

$$\frac{E^{n+1}_{y,k_x,k_y} - E^n_{y,k_x,k_y}}{\Delta t} = -ik_x B^{n+1/2}_{z,k_x,k_y} - J^{n+1/2}_{y,k_x,k_y}, \tag{15}$$

$$\frac{B^{n+1/2}_{z,k_x,k_y} - B^{n-1/2}_{z,k_x,k_y}}{\Delta t} = ik_y E^n_{x,k_x,k_y} - ik_x E^n_{y,k_x,k_y}. \tag{16}$$

The discrete spectral Gauss' law at time t^n writes

$$ik_x E^n_{x,k_x,k_y} + ik_y E^n_{y,k_x,k_y} = \rho^n_{k_x,k_y}. \tag{17}$$

Taking the discrete Ampère law in the spectral case, amounts to summing (14) multiplied by ik_x and (15) multiplied by ik_y. This leads to

$$\frac{1}{\Delta t}(ik_x E^{n+1}_{x,k_x,k_y} + ik_y E^{n+1}_{y,,k_x,k_y} - ik_x E^n_{x,k_x,k_y} - ik_y E^n_{y,k_x,k_y}) = -(ik_x J^{n+1/2}_{x,k_x,k_y} + ik_y J^{n+1/2}_{y,k_x,k_y}).$$

Notice that here also, like in the Yee scheme the discrete curl of B_z vanishes in the last equation, which is a necessary property for our Maxwell solvers if we want a discrete continuity equation. Since the Gauss law (17) is satisfied at time t^n, we then have

$$ik_x E^{n+1}_{x,k_x,k_y} + ik_y E^{n+1}_{y,k_x,k_y} = \rho^n_{k_x,k_y} - \Delta t(ik_x J^{n+1/2}_{x,k_x,k_y} + ik_y J^{n+1/2}_{y,k_x,k_y}). \tag{18}$$

The discrete version of the continuity equation (7) reads here

$$\rho^{n+1}_{k_x,k_y} = \rho^n_{k_x,k_y} - \Delta t(ik_x J^{n+1/2}_{x,k_x,k_y} + ik_y J^{n+1/2}_{y,k_x,k_y}). \tag{19}$$

If this is ensured, if follows from (18) that

$$ik_x E^{n+1}_{x,k_x,k_y} + ik_y E^{n+1}_{y,k_x,k_y} = \rho^{n+1}_{k_x,k_y},$$

which is the Gauss law is satisfied at time t^{n+1}.

3. Computation of the discrete charge and current density from the Vlasov solver compatible with the discrete continuity equation

Having identified the discrete continuity equation for the Maxwell solver that we want to use, the next task is to find a way to compute the discrete charge and current densities from the Vlasov equation so that they satisfy this discrete continuity equation.

For Particle In Cell (PIC) Vlasov solvers associated to the Yee Maxwell solver there is a well-known procedure for doing that introduced by Villasenor and Buneman [16] generalised to higher order deposition schemes in [2, 1]. Other options are also possible, like those introduced by Esirkepov [11], Umeda [15] or Chen et al. [4].

In the case of grid based Vlasov solvers, Sircombe and Arber [14] showed that this could be enforced for a split-eulerian Vlasov solver using the PPM method of Colella and Woodward [5] by computing $\mathbf{J}$ from the fluxes needed by the algorithm in the configuration space advections. Let us now show that this idea can be applied for general Finite Volume schemes, including as we will see conservative semi-Lagrangian schemes, following [9].

A splitting of the Vlasov equation between configuration space and velocity space advection will lead us to solve alternatively

$$\frac{\partial f}{\partial t} + \mathbf{v} \cdot \nabla_{\mathbf{x}} f = 0, \tag{20}$$

and

$$\frac{\partial f}{\partial t} + (\mathbf{E}(t, \mathbf{x}) + \mathbf{v} \times \mathbf{B}(t, \mathbf{x})) \cdot \nabla_{\mathbf{v}} f = 0, \tag{21}$$

The second equation does not modify ρ as can be seen integrating with respect to the velocity $\mathbf{v}$. Hence it should not provide any direct contribution to $\mathbf{J}$ either for the discrete continuity equation to be satisfied. We shall only require that the discrete solver exactly conserves ρ at all spatial grid points, which is the case for all conservative solvers. So assuming a conservative solver is used for the velocity space advection, our problem is now to design a configuration space advection compatible with the discrete continuity equation given by the Maxwell solver.

We first notice that the advection in configuration space (20) is for each given $\mathbf{v}$ via constant coefficient advection. Note that this would be true also in the relativistic case for each given $\mathbf{p}$.

We shall further split the configuration space advection for fixed $\mathbf{v}$ into two 1D advections (in x and y directions), which is simpler and less costly.

Note that this does not introduce an additional splitting error as constant coefficient advections commute.

Finally, we only need to consider constant coefficient 1D advections of the form

$$\frac{\partial f}{\partial t} + a\frac{\partial f}{\partial x} = 0, \tag{22}$$

with a being v_x or v_y at a given velocity grid point.

We shall provide compatible schemes in the case of the Finite Volumes and spectral methods we consider.

3.1. Finite volume schemes

Let us define uniformly spaced control cells $[x_{i-1/2}, x_{i+1/2}]$ with $x_{i+1/2} - x_{i-1/2} = \Delta x$. The unknown in a Finite Volume scheme will be the average value on a control cell that we shall denote by

$$f_i = \frac{1}{\Delta x}\int_{x_{i-1/2}}^{x_{i+1/2}} f(x)\,dx.$$

Integrating (22) on a control cell and between time t^n and t^{n+1} yields

$$f_i^{n+1} = f_i^n - \frac{a}{\Delta x}\int_{t^n}^{t^{n+1}} (f(t, x_{i+1/2}) - f(t, x_{i-1/2}))\,dt.$$

Let us denote by $f_{i+1/2}^{n+1/2}$ a numerical approximation of $\frac{1}{\Delta t}\int_{t^n}^{t^{n+1}} f(t, x_{i+1/2})\,dt$. Then our Finite Volume scheme becomes

$$f_i^{n+1} = f_i^n - \frac{a\Delta t}{\Delta x}(f_{i+1/2}^{n+1/2} - f_{i-1/2}^{n+1/2}). \tag{23}$$

Note that the actual computation of $f_{i+1/2}^{n+1/2}$ makes up the specific Finite Volume scheme, this could be done with an upwind scheme or the PPM scheme or others. For our purposes, it will be sufficient to consider this generic form of the Finite Volume scheme.

Let us now come back to our split Vlasov solver, for which a Finite Volume scheme of the form (23) will be used in the x and y advection steps and any conservative scheme in the $\mathbf{v}$ advection step. We discretize the distribution function on a 4D grid with uniform steps in each direction, denoting by i the

x index, j the y index, k the v_x index and ℓ the v_y index such that $f^n_{i,j,k,\ell} \simeq f(t^n, x_i, y_j, v_{x_k}, v_{y_\ell})$. Starting from $f^n_{i,j,k,\ell}$ at time step t^n, the algorithm reads,

$$
\begin{aligned}
f^{n,1}_{i,j,k,\ell} &= f^n_{i,j,k,\ell} - \frac{v_{x_k}\Delta t}{2\Delta x}(f^{n,1/2}_{i+1/2,j,k,\ell} - f^{n,1/2}_{i-1/2,j,k,\ell}),\\
f^{n,2}_{i,j,k,\ell} &= f^{n,1}_{i,j,k,\ell} - \frac{v_{y_\ell}\Delta t}{2\Delta y}(f^{n,3/2}_{i,j+1/2,k,\ell} - f^{n,3/2}_{i,j-1/2,k,\ell}),\\
f^{n,3}_{i,j,k,\ell} &\leftarrow f^{n,2}_{i,j,k,\ell} \text{ using a conservative advection in } \mathbf{v} \text{ space},\\
f^{n,4}_{i,j,k,\ell} &= f^{n,3}_{i,j,k,\ell} - \frac{v_{y_\ell}\Delta t}{2\Delta y}(f^{n,7/2}_{i,j+1/2,k,\ell} - f^{n,7/2}_{i,j-1/2,k,\ell}),\\
f^{n+1}_{i,j,k,\ell} &= f^{n,4}_{i,j,k,\ell} - \frac{v_{x_k}\Delta t}{2\Delta x}(f^{n,9/2}_{i+1/2,j,k,\ell} - f^{n,9/2}_{i-1/2,j,k,\ell}).
\end{aligned}
$$

Now, the discrete charge density is linked to the discrete distribution function by

$$\rho^n_{i,j} = \Delta v_x \Delta v_y \sum_k \sum_\ell f^n_{i,j,k,\ell},$$

where $\Delta v_x = (v_{x,\max} - v_{x,\min})/N_{v_x}$ (resp. $\Delta v_y = (v_{y,\max} - v_{y,\min})/N_{v_y}$) denotes the velocity step in the v_x (resp. v_y) direction. So, using the previous algorithm we can relate $\rho^{n+1}_{i,j}$ to $\rho^n_{i,j}$ by summing the different lines with respect to k, ℓ. Then, we get

$$
\begin{aligned}
\frac{1}{\Delta v_x \Delta v_y}\rho^{n+1}_{i,j} &= \sum_{k,\ell} f^{n+1}_{i,j,k,\ell}\\
&= \sum_{k,\ell} f^{n,4}_{i,j,k,\ell} - \frac{\Delta t}{2\Delta x}\sum_{k,\ell} v_{x_k}(f^{n,9/2}_{i+1/2,j,k,\ell} - f^{n,9/2}_{i-1/2,j,k,\ell})\\
&= \sum_{k,\ell} f^{n,3}_{i,j,k,\ell} - \frac{\Delta t}{2\Delta y}\sum_{k,\ell} v_{y_\ell}(f^{n,7/2}_{i,j+1/2,k,\ell} - f^{n,7/2}_{i,j-1/2,k,\ell})\\
&\qquad - \frac{\Delta t}{2\Delta x}\sum_{k,\ell} v_{x_k}(f^{n,9/2}_{i+1/2,j,k,\ell} - f^{n,9/2}_{i-1/2,j,k,\ell})
\end{aligned}
$$

Then the conservativity of the advection in $\mathbf{v}$ space yields $\sum_{k,\ell} f^{n,3}_{i,j,k,\ell} = \sum_{k,\ell} f^{n,2}_{i,j,k,\ell}$. Thus, proceeding in the same manner with the first two steps of

the algorithm we finally get

$$\begin{aligned}\frac{1}{\Delta v_x \Delta v_y}\rho_{i,j}^{n+1} &= \sum_{k,\ell} f_{i,j,k,\ell}^{n} \\ &-\frac{\Delta t}{2\Delta y}\sum_{k,\ell} v_{y_\ell}(f_{i,j+1/2,k,\ell}^{n,7/2} + f_{i,j+1/2,k,\ell}^{n,3/2} - f_{i,j-1/2,k,\ell}^{n,7/2} - f_{i,j-1/2,k,\ell}^{n,3/2}) \\ &-\frac{\Delta t}{2\Delta y}\sum_{k,\ell} v_{x_k}(f_{i+1/2,j,k,\ell}^{n,9/2} + f_{i+1/2,j,k,\ell}^{n,1/2} - f_{i-1/2,j,k,\ell}^{n,9/2} - f_{i-1/2,j,k,\ell}^{n,1/2}). \end{aligned} \quad (24)$$

Let us know denote by

$$J_{x_{i+1/2,j}}^{n+1/2} = \Delta v_x \Delta v_y \sum_{k,\ell} v_{x_k} \frac{1}{2}(f_{i+1/2,j,k,\ell}^{n,9/2} + f_{i+1/2,j,k,\ell}^{n,1/2}), \quad (25)$$

$$J_{y_{i,j+1/2}}^{n+1/2} = \Delta v_x \Delta v_y \sum_{k,\ell} v_{y_\ell} \frac{1}{2}(f_{i,j+1/2,k,\ell}^{n,7/2} + f_{i,j+1/2,k,\ell}^{n,3/2}). \quad (26)$$

Then (24) becomes

$$\frac{\rho_{i,j}^{n+1} - \rho_{i,j}^{n}}{\Delta t} + \frac{J_{x_{i+1/2,j}}^{n+1/2} - J_{x_{i-1/2,j}}^{n+1/2}}{\Delta x} + \frac{J_{y_{i,j+1/2}}^{n+1/2} - J_{y_{i,j-1/2}}^{n+1/2}}{\Delta y} = 0,$$

which is exactly the discrete continuity equation (13) needed by the Yee scheme. Hence expressions (25)-(26) provide an expression of the discrete current density **J** consistent with a Finite Volume Vlasov solver and that satisfies a discrete continuity equation.

3.2. Finite Volume form of a semi-Lagrangian scheme

We have obtained in the previous section an explicit expression for the discrete current which satisfies a discrete continuity equation for any split Vlasov solver for which the x and y advection parts can be cast in the generic Finite Volume framework (23). We are now going to cast a conservative semi-Lagrangian scheme [9] for constant coefficient advection into this Finite Volume formalism. This will then enable us to construct charge conserving algorithms for a large class of split semi-Lagrangian schemes.

In both Finite Volume and conservative semi-Lagrangian schemes, the first step is to reconstruct a piecewise polynomial function on each cell. We shall call f^R this reconstructed piecewise polynomial function. The reconstruction scheme does not matter for our purpose, it could be PPM, splines

or something else, with limiters or not. The only property we shall need is that it is linked to the computed cell averages $f_i^n = \frac{1}{\Delta x}\int_{x_{i-1/2}}^{x_{i+1/2}} f(t^n,x)\,dx$, by

$$f_i^n = \frac{1}{\Delta x}\int_{x_{i-1/2}}^{x_{i+1/2}} f^R(x)\,dx.$$

We shall also assume that the CFL condition $\frac{a\Delta t}{\Delta x} \leq 1$ is verified.

In a Finite Volume scheme for the 1D advection equation (22), we then compute

$$\begin{aligned} f_{i+1/2}^{n+1/2} &= \frac{1}{\Delta t}\int_{t^n}^{t^{n+1}} f(t,x_{i+1/2})\,dt \\ &= \frac{1}{\Delta t}\int_{t^n}^{t^{n+1}} f(t^n,x_{i+1/2}-a(t-t^n))\,dt \\ &\simeq \frac{1}{\Delta t}\int_{t^n}^{t^{n+1}} f^R(x_{i+1/2}-a(t-t^n))\,dt, \end{aligned}$$

and by the change of variables $x = x_{i+1/2} - a(t-t^n)$

$$f_{i+1/2}^{n+1/2} = \frac{1}{a\Delta t}\int_{x_{i+1/2}-a\Delta t}^{x_{i+1/2}} f^R(x)\,dx.$$

Then using the formulation (23), we get the Finite Volume scheme

$$f_i^{n+1} = f_i^n - \frac{1}{\Delta x}\left(\int_{x_{i+1/2}-a\Delta t}^{x_{i+1/2}} f^R(x)\,dx - \int_{x_{i-1/2}-a\Delta t}^{x_{i-1/2}} f^R(x)\,dx\right). \qquad (27)$$

On the other hand, for a conservative semi-Lagrangian scheme, the distribution function is updated using the relation

$$f_i^{n+1} = \frac{1}{\Delta x}\int_{X(x_{i-1/2})}^{X(x_{i-1/2})} f^R(x)\,dx,$$

where $X(x_{i+1/2})$ is the origin of the characteristic ending at $x_{i+1/2}$, that is in our case of constant advection at velocity a, $X(x_{i+1/2}) = x_{i+1/2} - a\Delta t$.

Hence

$$
\begin{aligned}
f_i^{n+1} &= \frac{1}{\Delta x}\int_{x_{i-1/2}-a\Delta t}^{x_{i+1/2}-a\Delta t} f^R(x)\,dx \\
&= \frac{1}{\Delta x}\left(\int_{x_{i-1/2}-a\Delta t}^{x_{i-1/2}} f^R(x)\,dx + \int_{x_{i-1/2}}^{x_{i+1/2}} f^R(x)\,dx - \int_{x_{i+1/2}-a\Delta t}^{x_{i+1/2}} f^R(x)\,dx\right) \\
&= f_i^n + \frac{1}{\Delta x}\left(\int_{x_{i-1/2}-a\Delta t}^{x_{i-1/2}} f^R(x)\,dx - \int_{x_{i+1/2}-a\Delta t}^{x_{i+1/2}} f^R(x)\,dx\right)
\end{aligned}
$$

which is the same expression as (27), so that both formalisms yield the same numerical scheme. Moreover, the finite volume flux $f_{i+1/2}^{n+1/2}$ can be expressed for a semi-Lagrangian scheme with respect to the reconstructed function f^R by

$$
f_{i+1/2}^{n+1/2} = \frac{1}{a\Delta t}\int_{x_{i+1/2}-a\Delta t}^{x_{i+1/2}} f^R(x)\,dx.
$$

In particular, if the reconstruction is performed using a primitive F^R of f^R, we have

$$
f_{i+1/2}^{n+1/2} = \frac{1}{a\Delta t}\left(F^R(x_{i+1/2}) - F^R(x_{i+1/2}-a\Delta t)\right).
$$

It now remains to provide the fluxes for both half advections in x and y. For the half-advections in x, we have on the one hand, integrating on $[t^n, t^{n+1/2}]\times[x_{i-1/2}, x_{i+1/2}]$

$$
\begin{aligned}
f_i^{n,1} &= f_i^n - \frac{v_x\Delta t}{2\Delta x}\int_{t^n}^{t^{n+1/2}} \left[f(t,x_{i+1/2}) - f(t,x_{i+1/2})\right]dt \\
&= f_i^n - \frac{v_x\Delta t}{2\Delta x}\left[f_{i+1/2}^{n,1/2} - f_{i-1/2}^{n,1/2}\right], \qquad (28)
\end{aligned}
$$

with $f_{i+1/2}^{n,1/2} = \int_{t^n}^{t^{n+1/2}} f(t,x_{i+1/2})dt$. On the other hand

$$
\begin{aligned}
f_i^{n,1} &:= \frac{1}{\Delta x}\int_{x_{i-1/2}}^{x_{i+1/2}} f^{n,1}(x)dx \\
&= \frac{1}{\Delta x}\int_{x_{i-1/2-v_x\Delta t/2}}^{x_{i+1/2}-v_x\Delta t/2} f^n(x)dx \\
&= f_i^n - \frac{1}{\Delta x}(\phi_{i+1/2}^{n,1/2} - \phi_{i-1/2}^{n,1/2}), \qquad (29)
\end{aligned}
$$

where $\phi_{i+1/2}^{n,1/2} = \int_{x_{i+1/2}}^{x_{i+1/2}-v_x\Delta t/2} f^n(x)dx$. Hence, we can identify the fluxes in (28) and (29) to get

$$f_{i+1/2}^{n,1/2} = \begin{cases} \phi_{i+1/2}^{n,1/2}/(v_x\Delta t/2) & \text{if } v_x \neq 0, \\ 0 & \text{if } v_x = 0. \end{cases}$$

In the same way for $f_{i+1/2}^{n,9/2}$, we have

$$f_{i+1/2}^{n,9/2} = \begin{cases} \phi_{i+1/2}^{n,9/2}/(v_x\Delta t/2) & \text{if } v_x \neq 0, \\ 0 & \text{if } v_x = 0. \end{cases}$$

Then, it comes

$$\begin{aligned} \phi_{i+1/2}^{n,1/2} &= F^R(x_{i+1/2}) - F^R(x_{i+1/2} - v_x\Delta t/2) \text{ with } F^R \text{ the primitive of } f^n, \\ \phi_{i+1/2}^{n,9/2} &= F^R(x_{i+1/2}) - F^R(x_{i+1/2} - v_x\Delta t/2) \text{ with } F^R \text{ the primitive of } f^{n,4}. \end{aligned}$$

For the half-advections in y, we proceed in the same way integrating on $[t^n, t^{n+1/2}] \times [y_{j-1/2}, y_{j+1/2}]$ in order to obtain the finite volume formulation (as (28)) and identifying with the conservative semi-Lagrangian formulation (as (29)), we have

$$f_{j+1/2}^{n,3/2} = \begin{cases} \phi_{j+1/2}^{n,3/2}/(v_y\Delta t/2) & \text{if } v_y \neq 0, \\ 0 & \text{if } v_y = 0. \end{cases}$$

and

$$f_{j+1/2}^{n,7/2} = \begin{cases} \phi_{j+1/2}^{n,7/2}/(v_y\Delta t/2) & \text{if } v_y \neq 0, \\ 0 & \text{if } v_y = 0. \end{cases}$$

Then, we get similarly

$$\begin{aligned} \phi_{j+1/2}^{n,3/2} &= F^R(y_{j+1/2}) - F^R(y_{j+1/2} - v_y\Delta t/2) \text{ with } F^R \text{ the primitive of } f^{n,1}, \\ \phi_{j+1/2}^{n,7/2} &= F^R(y_{j+1/2}) - F^R(y_{j+1/2} - v_y\Delta t/2) \text{ with } F^R \text{ the primitive of } f^{n,3}. \end{aligned}$$

3.3. Spectral scheme

Denoting by $f^n(k_x, k_y, v_x, v_y)$ the Fourier transform in space of $f(t^n)$, the 1D advections in configuration space become for the spectral scheme

$$\frac{\partial f}{\partial t} + ik_x v_x f = 0, \tag{30}$$

for which the exact solution on a time step reads $f(t+\Delta t) = f(t)\exp(-ik_x v_x \Delta t)$, and the same for the advection in y.

So, using a spectral scheme in space coupled with a Strang splitting, we get the following algorithm

$$
\begin{aligned}
&f^{n,1}_{k_x,k_y,k,\ell} = f^{n}_{k_x,k_y,k,\ell}\exp(-ik_x v_x \Delta t/2),\\
&f^{n,2}_{k_x,k_y,k,\ell} = f^{n,1}_{k_x,k_y,k,\ell}\exp(-ik_y v_y \Delta t/2),\\
&f^{n,3}_{k_x,k_y,k,\ell} \leftarrow f^{n,2}_{k_x,k_y,k,\ell} \text{ using a conservative advection in } \mathbf{v} \text{ space},\\
&f^{n,4}_{k_x,k_y,k,\ell} = f^{n,3}_{k_x,k_y,k,\ell}\exp(-ik_y v_y \Delta t/2),\\
&f^{n+1}_{k_x,k_y,k,\ell} = f^{n,4}_{k_x,k_y,k,\ell}\exp(-ik_x v_x \Delta t/2).
\end{aligned}
$$

As we did for the Finite Volume schemes, we need to extract the current from the space advections in a way that is compatible with the discrete continuity equation (19) for the Maxwell solver we want to couple to. To this aim we need to make a transport structure appear. Introducing $f^{n,1/2}_{k_x,k_y,k,\ell}$

$$
f^{n,1/2}_{k_x,k_y,k,\ell} = \begin{cases} f^{n}_{k_x,k_y,k,\ell}\left[1-\exp(-ik_x v_x \Delta t/2)\right]/(ik_x \Delta t/2) & \text{if } k_x \neq 0,\\ 0 & \text{if } k_x = 0, \end{cases} \tag{31}
$$

the first advection in x writes

$$
f^{n,1}_{k_x,k_y,k,\ell} = f^{n}_{k_x,k_y,k,\ell} - ik_x \frac{\Delta t}{2} f^{n,1/2}_{k_x,k_y,k,\ell}.
$$

Using the same notations, one has for the last x-advection

$$
f^{n+1}_{k_x,k_y,k,\ell} = f^{n,4}_{k_x,k_y,k,\ell} - ik_x \frac{\Delta t}{2} f^{n,9/2}_{k_x,k_y,k,\ell},
$$

where $f^{n,9/2}$ is deduced from (31) by replacing f^n by $f^{n,4}$. Similarly, for the y-advections, it comes

$$
\begin{aligned}
f^{n,2}_{k_x,k_y,k,\ell} &= f^{n,1}_{k_x,k_y,k,\ell} - ik_y \frac{\Delta t}{2} f^{n,3/2}_{k_x,k_y,k,\ell},\\
f^{n,4}_{k_x,k_y,k,\ell} &= f^{n,3}_{k_x,k_y,k,\ell} - ik_y \frac{\Delta t}{2} f^{n,7/2}_{k_x,k_y,k,\ell},
\end{aligned}
$$

where $f^{n,3/2}$ (resp. $f^{n,7/2}$) is given by the following expression with $d=0$ (resp. $d=2$)

$$
f^{n,d+3/2}_{k_x,k_y,k,\ell} = \begin{cases} f^{n,(d+1)}_{k_x,k_y,k,\ell}\left[1-\exp(-ik_y v_y \Delta t/2)\right]/(ik_y \Delta t/2) & \text{if } k_y \neq 0,\\ 0 & \text{if } k_y = 0. \end{cases} \tag{32}
$$

Now, let us add up the different contributions to the current. First, the discrete charge density is linked to the discrete distribution function by

$$\rho^n_{k_x,k_y} = \Delta v_x \Delta v_y \sum_k \sum_\ell f^n_{k_x,k_y,k,\ell}.$$

So, using the previous algorithm we can relate $\rho^{n+1}_{k_x,k_y}$ to $\rho^n_{k_x,k_y}$ by summing the different lines with respect to k, ℓ. Then, we get

$$\begin{aligned}
\frac{1}{\Delta v_x \Delta v_y} \rho^{n+1}_{k_x,k_y} &= \sum_{k,\ell} f^{n+1}_{k_x,k_y,k,\ell} \\
&= \sum_{k,\ell} \left[f^{n,4}_{k_x,k_y,k,\ell} - ik_x \frac{\Delta t}{2} f^{n,9/2}_{k_x,k_y,k,\ell} \right] \\
&= \sum_{k,\ell} \left[f^{n,3}_{k_x,k_y,k,\ell} - ik_y \frac{\Delta t}{2} f^{n,7/2}_{k_x,k_y,k,\ell} - ik_x \frac{\Delta t}{2} f^{n,9/2}_{k_x,k_y,k,\ell} \right].
\end{aligned}$$

Then the conservativity of the advection in $\mathbf{v}$ space yields $\sum_{k,\ell} f^{n,3}_{k_x,k_y,k,\ell} = \sum_{k,\ell} f^{n,2}_{k_x,k_y,k,\ell}$. Thus, proceeding in the same manner with the first two steps of the algorithm we finally get

$$\begin{aligned}
\frac{1}{\Delta v_x \Delta v_y} \rho^{n+1}_{k_x,k_y} = \sum_{k,\ell} f^n_{k_x,k_y,k,\ell} &- ik_y \frac{\Delta t}{2} \sum_{k,\ell} (f^{n,7/2}_{k_x,k_y,k,\ell} + f^{n,3/2}_{k_x,k_y,k,\ell}) \\
&- ik_x \frac{\Delta t}{2} \sum_{k,\ell} (f^{n,9/2}_{k_x,k_y,k,\ell} + f^{n,1/2}_{k_x,k_y,k,\ell}). \quad (33)
\end{aligned}$$

Let us now denote by

$$J^{n+1/2}_{x,k_x,k_y} = \Delta v_x \Delta v_y \sum_{k,\ell} \frac{1}{2} (f^{n,9/2}_{k_x,k_y,k,\ell} + f^{n,1/2}_{k_x,k_y,k,\ell}), \quad (34)$$

$$J^{n+1/2}_{y,k_x,k_y} = \Delta v_x \Delta v_y \sum_{k,\ell} \frac{1}{2} (f^{n,7/2}_{k_x,k_y,k,\ell} + f^{n,3/2}_{k_x,k_y,k,\ell}). \quad (35)$$

Then (33) becomes

$$\frac{\rho^{n+1}_{k_x,k_y} - \rho^n_{k_x,k_y}}{\Delta t} + ik_x J^{n+1/2}_{x,k_x,k_y} + ik_y J^{n+1/2}_{k_x,k_y} = 0,$$

which is exactly the discrete continuity equation (19) needed by the spectral Maxwell scheme.

Hence expressions (34)-(35) provide an expression of the discrete current density **J** consistent with a spectral Vlasov solver and that satisfies a discrete continuity equation.

4. Reconstruction

In this section, we recall the different reconstructions we used in this work. Let apply the conservative method to the following problem, using the notations introduced in the previous sections

$$\partial_t f + a\partial_x f = 0.$$

Introducing the primitive function $F(x) = \int_{x_{-1/2}}^{x} f(y)dy$, the conservative numerical scheme is

$$\begin{aligned} f_i^{n+1} &= \frac{1}{\Delta x}\int_{x_{i-1/2}-a\Delta t}^{x_{i+1/2}-a\Delta t} f(t^n,y)dy \\ &= \frac{1}{\Delta x}[F(x_{i+1/2}-a\Delta t) - F(x_{i-1/2}-a\Delta t)] \\ &= f_i^n - \frac{1}{\Delta x}[F(x_{i+1/2}) - F(x_{i+1/2}-a\Delta t) - F(x_{i-1/2}) - F(x_{i-1/2}-a\Delta t)]. \end{aligned}$$

The interpolation conditions for the primitive are $F(x_{i+1/2}) = \sum_{j=0}^{i} f_j^n$ and we need to reconstruct the primitive F to evaluate at $x_{i\pm1/2} - a\Delta t$. Following [9], we use a Hermite reconstruction. If the feet of the characteristics satisfies $x_{i+1/2} - a\Delta t \in [x_{j-1/2}, x_{j+1/2}[$, we denote by $x \in [0,1[$ $x = x_{i+1/2} - a\Delta t - x_{j-1/2}$ and the reconstruction writes for $x \in [0,1[$

$$\begin{aligned} F(x_{i+1/2}-a\Delta t) &= F(x_{j-1/2})(1-x)^2(1+2x) + F(x_{j+1/2})x^2(3-2x) \\ &\quad + F'(x_{j-1/2})x(1-x)^2 + F'(x_{j+1/2})x^2(x-1). \end{aligned}$$

To approximate the derivative F', we use the following formula leading to different numerical schemes

$$\begin{aligned} F'(x_{j-1/2}) &= \frac{7}{12}(f_{j+1}+f_j) - \frac{1}{12}(f_{j+2}+f_{j-1}) \quad \text{(PPM1)} \\ F'(x_{j-1/2}) &= \frac{1}{60}(f_{j+3} - f_{j-3} + 9(f_{j-2}-f_{j+2}) + 45(f_{j+1}-f_{j-1})) \quad \text{(PPM2)} \\ F'(x_{j+1/2}) &= \frac{1}{6}(5f_j + 2f_{j+1} - f_{j-1}), \quad F'(x_{j-1/2}) = \frac{1}{6}(5f_j - f_{j+1} + 2f_{j-1}) \quad \text{(LAG3).} \end{aligned}$$

For more details, see [9]. Let us remark that high order upwind reconstruction LAG$(2d+1)$ and the extension to the two dimensional case are possible (see [8]).

5. Coupling the Vlasov solver with the Maxwell solver

The only point that is not straightforward in the coupling of our Vlasov solvers with their corresponding Maxwell solvers, is how to get the electric field $E^{n+1/2}$, needed for the velocity space advection before the full current has been computed. We use here for both our methods the strategy suggested in [14]. Ampère is advanced on $\Delta t/2$ using the predict currents J^n computed using

$$J^n_{x,i+1/2,j} = \Delta v_x \Delta v_y \sum_{k,\ell} \frac{v_{x_k}}{2} (f^n_{i,j,k,\ell} + f^n_{i+1,j,k,\ell}), \tag{36}$$

$$J^n_{y,i,j+1/2} = \Delta v_x \Delta v_y \sum_{k,\ell} \frac{v_{y_k}}{2} (f^n_{i,j,k,\ell} + f^n_{i,j+1,k,\ell}). \tag{37}$$

This predicted electric field is then only used for the velocity advection and discarded. The electric field E^{n+1} will later be recomputed directly from E^n using the current $J^{n+1/2}$ verifying the discrete continuity equation.

Another point comes from the fact that, before the advection in $\mathbf{v}$, we have the electric field on staggered grid $E^{n+1/2}_{x_{i+1/2,j}}$, $E^{n+1/2}_{y_{i,j+1/2}}$ whereas we need it at the grid points (x_i, y_j). A simple average enables to compute $E^{n+1/2}_{x_{i,j}}$, $E^{n+1/2}_{y_{i,j}}$.

Finally, the initialization has to be done carefully. Indeed, one has to initialize f^0 such that its density ρ^0 satisfies the appropriate discrete Gauss law. In practice, for a given initial condition f^0, we compute ρ^0 and solve the Poisson equation to get (E^0_x, E^0_y) using any solvers. Then, ρ^0 is modified in such a way that it solves exactly the appropriate discrete Gauss law. Once ρ^0 is re-computed, f^0 is modified according to ρ^0.

We then get in both cases the following algorithm where the half advections in x and y need to use the adequate formula for each solver introduced previously.

Algorithm. Starting from $E^n = (E^n_x, E^n_y)$, $B^{n-1/2}_z$ and f^n, we compute E^{n+1}, $B^{n+1/2}_z$ and f^{n+1} as

1. Maxwell prediction $\rightarrow B_z^{n+1/2}$ and $(E_x^{n+1/2}, E_y^{n+1/2})$
   (a) advance Faraday (16) on Δt with $B_z^{n-1/2}$ and $E^n \rightarrow B_z^{n-1/2}$
   (b) compute $J_x^n = \sum_{k,\ell} v_{x_k} f^n \Delta v_x \Delta v_y$ and $J_y^n = \sum_{k,\ell} v_{y_\ell} f^n \Delta v_x \Delta v_y$.
   (c) advance Ampère (14)-(15) on $\Delta t/2$ with E^n, $B_z^{n+1/2}$ and (J_x^n, J_y^n) $\rightarrow E^{n+1/2}$
2. half-advection in x $\rightarrow f^{n,1}$ and $J_x^{n,1/2}$
   (a) compute $f^{n,1/2}$ and $J_x^{n,1/2} = \sum_{k,\ell} v_{x_k} f^{n,1/2} \Delta v_x \Delta v_y$
   (b) half-advection in x.
3. half-advection in y $\rightarrow f^{n,2}$ et $J_y^{n,3/2}$
   (a) compute $f^{n,3/2}$ and $J_y^{n,3/2} = \sum_{k,\ell} v_{y_\ell} f^{n,3/2} \Delta v_x \Delta v_y$
   (b) half-advection in y.
4. advection in v with $E^{n+1/2}$ and $B_z^{n+1/2} \rightarrow f^{n,3}$
5. half-advection in y $\rightarrow f^{n,4}$ and $J_y^{n,7/2}$
   (a) compute $f^{n,7/2}$ and $J_y^{n,7/2} = \sum_{k,\ell} v_{y_\ell} f^{n,7/2} \Delta v_x \Delta v_y$
   (b) half-advection in y.
6. half-advection in x $\rightarrow f^{n+1}$ and $J_x^{n,9/2}$
   (a) compute $f^{n,9/2}$ and $J_x^{n,9/2} = \sum_{k,\ell} v_{x_k} f^{n,9/2} \Delta v_x \Delta v_y$
   (b) half-advection in x.
7. Advance Maxwell $\rightarrow E_x^{n+1}$ et E_y^{n+1}
   (a) compute $J_x^{n+1/2} = (J_x^{n,1/2} + J_x^{n,9/2})/2$
   (b) compute $J_y^{n+1/2} = (J_y^{n,3/2} + J_y^{n,7/2})/2$
   (c) advance Ampère (14)-(15) on Δt with E^n, $B_z^{n+1/2}$ and $(J_x^{n+1/2}, J_y^{n+1/2})$ $\rightarrow E^{n+1}$

6. Numerical results

We focus on classical test cases which have the advantage to be compared easily to a Vlasov-Poisson solver. Indeed, we consider the following class of initial conditions

$$f_0(\mathbf{x},\mathbf{v}) = \mathcal{E}(v)(1+\alpha g(x,y)),$$

where $g(x,y)$ is a periodic function and $\mathcal{E}(v)$ a velocity function. Typically, we choose for the equilibrium

$$\mathcal{E}(v) = \frac{1}{2\pi}e^{-|\mathbf{v}|^2/2}(\text{Landau}) \quad \text{and } \mathcal{E}(v) = \frac{1}{2\pi}e^{-|\mathbf{v}|^2/2}v_x^2 \ \ (\text{TSI}).$$

For the spatial dependency, we consider $g(x,y) = \cos(k_x x)$ ("1Dx" case) to recover the one dimensional case or $g(x,y) = \cos(k_x x)\cos(k_y y)$ ("PROD" case). The parameters are chosen as follows: $k_x = k_y = 0.5 = 2\pi/L_x = 2\pi/L_y$ where $L_x = [0, 4\pi]$ (resp. $L_y = [0, 4\pi]$) denotes the spatial domain in the x direction (resp. y direction). The domain in velocity is $\mathbf{v} \in [-8, 8]^2$ to ensure that the discrete integration in the $\mathbf{v}$ directions is sufficiently precise.

We compare the present algorithm to a Vlasov-Poisson algorithm (VP) in which the electric field is computed just before the v advection.

Spectral schemes. In Figures 2 and 3, we plot the time history of the electric energy $\|E_x(t)\|_{L^2}^2 + \|E_y(t)\|_{L^2}^2$ for the reference method (VP) and the "new" method (VM), in the Landau case ($\alpha = 10^{-3}$). Figure 4 shows the time evolution of the electric energy in the TSI case ($\alpha = 10^{-3}$).

One can observe that the two methods are superimposed, illustrating the equivalence of the two algorithms. In particular, we checked that the electric field computed by VM at time t^{n+1} and the density ρ^{n+1} (computed from f^{n+1}) solve the discrete Gauss law (which is spectral in this case) up to machine precision and up to the precision of the conservation of the $\mathbf{v}$ advection. Two other nice properties of the VM algorithm can be emphasized. First, the one-dimensional cases are preserved. Indeed, for the "1Dx" case, the electric field E_y stays to zero for all times, the same being true in the symmetric case "1Dy". Second, if the magnetic field B_z is zero at the initial time, this property remains true for all $t > 0$.

Conservative schemes. In this last part, numerical results obtained by the conservative methods are shown. The numerical parameters are chosen as previously. The properties described previously (symmetry between x and

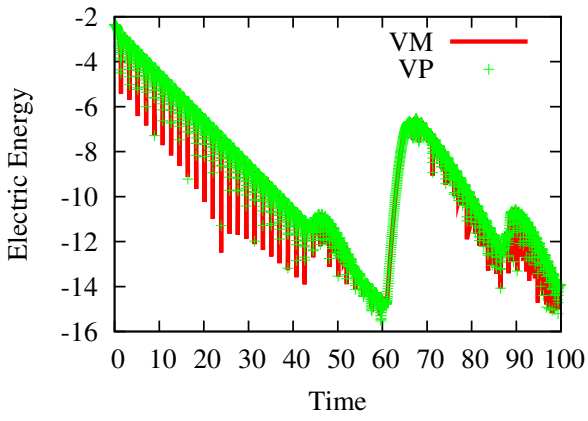

Figure 2: "PROD" case. Time history of the electric energy (semi log-scale): comparison of Vlasov-Poisson (VP) and Vlasov-Maxwell (VM). 64 points per spatial direction and 128 points per velocity direction. $\Delta t = 0.01$.

y and B_z equal to zero) are also verified in the conservative case. We compare the new algorithm for Vlasov-Maxwell with the Vlasov-Poisson in which the Gauss law is solved using a spectral solver. Hence, the two solvers are not equivalent since the Vlasov-Maxwell solver ensures the following discrete Gauss law

$$\frac{E^n_{x_{i+1/2,j}} - E^n_{x_{i-1/2,j}}}{\Delta x} + \frac{E^n_{y_{i,j+1/2}} - E^n_{y_{i,j-1/2}}}{\Delta y} = \rho^n_{i,j} - 1.$$

However, this difference is quite small and appears (see for example in Figure 6) when the amplitude of the electric energy is below a certain threshold. We can remark that the Vlasov-Maxwell solver benefits from the quality of the high order conservative methods used, which capture the long time behavior of the solution (see Figure 6) in a similar way as the spectral method. For a detailed comparison of these methods (regarding the conserved quantities), we refer to [9].

7. Conclusion

In this work, we have presented a class of Eulerian numerical schemes for the two dimensional Vlasov-Maxwell equations that ensure the discrete continuity equation, and as a consequence, the Gauss law. Moreover, since it is based on a directional splitting, this approach can benefit from an efficient

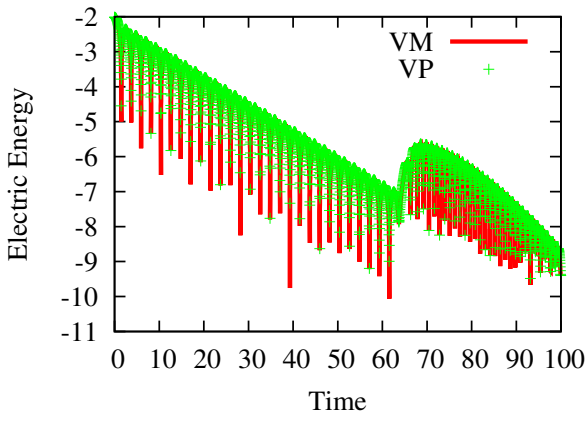

Figure 3: "1Dx" case. Time history of the electric energy (semi log-scale): comparison of Vlasov-Poisson (VP) and Vlasov-Maxwell (VM). 64 points per spatial direction and 128 points per velocity direction. $\Delta t = 0.01$.

parallelization using domain decomposition and transposition techniques (see [6]). Physically relevant numerical tests have to be performed; in particular, non periodic boundary conditions have to be adapted to the present approach. Also, higher order methods in time have to be studied to improve the accuarcy.

Acknowledgements. Computer time grants are kindly provided by the Rechenzentrum Garching (RZG).

[1] R. Barthelmé, *Le problème de conservation de la charge dans le couplage des équations de Vlasov et de Maxwell*, Thèse de l'Université Louis Pasteur, 2005.

[2] R. Barthelmé, C. Parzani, *Numerical charge conservation in particle-in-cell codes*, Numerical methods for hyperbolic and kinetic problems, IRMA Lect. Math. Theor. Phys. **7**, pp. 7-28, (2005).

[3] F. Bouchut, *On the discrete conservation of the Gauss-Poisson equation of plasma Physics*, Commun. Numer. Meth. Engng., pp. 23-34, (1998).

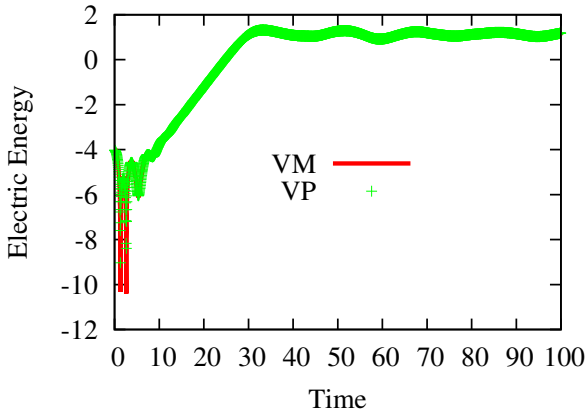

Figure 4: "TSI" case. Time history of the electric energy (semi log-scale): comparison of Vlasov-Poisson (VP) and Vlasov-Maxwell (VM). 64 points per spatial direction and 128 points per velocity direction. $\Delta t = 0.01$.

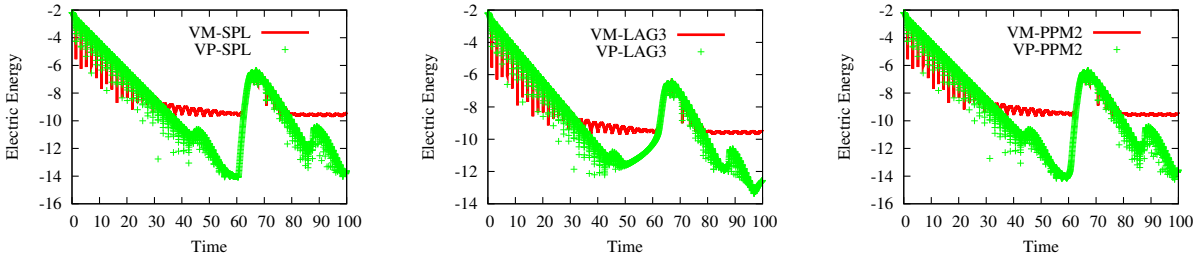

Figure 5: "PROD" case. Time history of the electric energy (semi log-scale): comparison of Vlasov-Poisson (VP) and Vlasov-Maxwell (VM). 64 points per spatial direction and 128 points per velocity direction. $\Delta t = 0.01$. From left to right: SPL, LAG3, PPM2.

[4] G. Chen, L. Chacón, D.C. Barnes, *An energy- and charge-conserving, implicit, electrostatic particle-in-cell algorithm*, J. Comput. Phys. **230**, pp. 7018-7036, (2011) .

[5] P. Colella, P.R. Woodward, *The Piecewise Parabolic Method (PPM) for gas-dynamical simulations*, J. Comput. Phys. **54**, pp. 174-201, (1984) .

[6] O. Coulaud, E. Sonnendrücker, E. Dillon, P. Bertrand, A. Ghizzo, *Parallelization of semi-Lagrangian Vlasov codes*, INRIA report 3430, 1998.

[7] N. Crouseilles, L. Einkemmer, E. Faou, *Hamiltonian splitting for the Vlasov-Maxwell equations*, submitted.

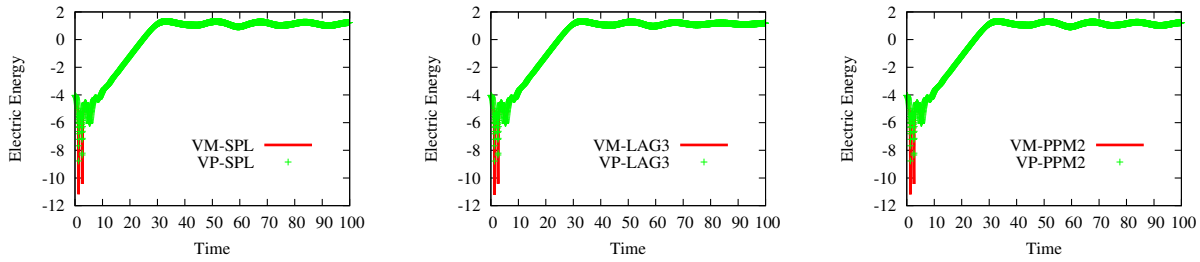

Figure 6: "TSI" case. Time history of the electric energy (semi log-scale): comparison of Vlasov-Poisson (VP) and Vlasov-Maxwell (VM). 64 points per spatial direction and 128 points per velocity direction. $\Delta t = 0.01$. From left to right: SPL, LAG3, PPM2.

[8] N. Crouseilles, P. Glanc, S. Hirstoaga, E. Madaule, M. Mehrenberger, J. Pétri, *Semi-Lagrangian simulations on polar grids: from diocotron instability to ITG turbulence*, submitted.

[9] N. Crouseilles, M. Mehrenberger, E. Sonnendrücker, *Conservative semi-Lagrangian schemes for the Vlasov equation*, J. Comput. Phys. **229**, pp. 1927-1953, (2010).

[10] N. Crouseilles, Th. Respaud, *A charge preserving scheme for the numerical resolution of the Vlasov-Ampère equations*, Comm. in Comput. Phys. **10**, pp. 1027-1043, (2011).

[11] T.Zh. Esirkepov, *Exact charge conservation scheme for Particle-in-Cell simulation with an arbitrary form-factor*, Comput. Phys. Comm. **135**, pp. 144-153, (2001).

[12] B. Marder, *A method for incorporating Gauss's law into electromagnetic PIC codes*, J. Comput. Phys. **68**, pp. 48-55, (1987).

[13] C.-D. Munz, R. Schneider, E. Sonnendrücker, U. Voss, *Maxwell's equations when the charge conservation is not satisfied*, C. R. Acad. Sci. Paris Sér. I Math. **328**, no. 5, pp. 431-436, (1999).

[14] N.J. Sircombe, T.D. Arber, *VALIS: A split-conservative scheme for the relativistic 2D*, J. Comput. Phys. **228**, pp. 4773-4788, (2009).

[15] T. Umeda, Y. Omura, T. Tominaga, H. Matsumoto, *A new charge conservation method in electromagnetic particle-in-cell simulations*, Comput. Phys. Commun. **156**, pp. 73-85, (2004).

[16] J. Villasenor, O. Buneman, *Rigorous charge conservation for local electromagnetic field solvers*, Comput. Phys. Commun. **69**, pp. 306-316, (1992).